Universal Nucleation Behavior of Sheared Systems

Amrita Goswami, Indranil Saha Dalal,* and Jayant K. Singh†
Department of Chemical Engineering, Indian Institute of Technology Kanpur, Kanpur, Uttar Pradesh 208016, India

(Received 8 January 2021; accepted 15 April 2021; published 12 May 2021)

Using molecular simulations and a modified classical nucleation theory, we study the nucleation, under flow, of a variety of liquids: different water models, Lennard-Jones, and hard sphere colloids. Our approach enables us to analyze a wide range of shear rates inaccessible to brute-force simulations. Our results reveal that the variation of the nucleation rate with shear is universal. A simplified version of the theory successfully captures the nonmonotonic temperature dependence of the nucleation behavior, which is shown to originate from the violation of the Stokes-Einstein relation.

DOI: 10.1103/PhysRevLett.126.195702

The nucleation of quiescent systems, at molecular scales, is of major interest and has been the focus of intense research [1]. However, in nature and in practice, static fluids are rarely involved; realistic systems almost always exist in a state of flux. The study of the effects of shear on nucleation is a burgeoning field, with far-reaching implications for industry and several branches of science. Despite investigations in this direction, the literature is rife with controversial results. Some studies indicate that the presence of shear inhibits the nucleation rate [2,3], while others assert that the nucleation rate is enhanced by shear [4–10]. A nonmonotonic dependence of the induction times for nucleation has also been reported in experiments [11,12].

The homogeneous nucleation of the sheared Ising model [13], colloidal models [14,15], hard spheres (HS) [16–18], glassy systems [19,20], a binary-alloy [21], and more recently mW water under shear [22,23], has been studied using theory and simulations. Water is a highly anomalous liquid exhibiting several anomalies in the supercooled regime [24], but efforts have not been made to distinguish the nature of the shear-dependent nucleation behavior of water, or to generalize shared traits. However, existing literature implies that the nucleation rate for liquids, including water, is nonmonotonic with shear [14–23].

In this Letter, we generalize the phenomenon of shear-induced nucleation by revealing the underlying universality of the same. Recently, we formulated a classical nucleation theory (CNT), extended to explicitly incorporate shear [23]. Here, we show the generality of this approach (henceforth referred to as "shear-CNT"), using it to explain the effects of shear on various systems: the rigid water models TIP4P/2005 [25], TIP4P/Ice [26], the coarse-grained mW water model [27], the Lennard-Jones (LJ) fluid [28], and a HS colloid. We examine, in detail, the dual effects of temperature and shear on the nucleation rates for water and LJ fluid, explore the provenance of anomalies, and highlight the universality in the nucleation behavior.

The free energy of a crystal nucleus in a bulk homogeneous nucleating system, under the effect of a simple volume-preserving shear $\dot{\gamma}$, is given by [17]

$$F(R) = -\frac{4}{3}\pi R^3 \frac{|\Delta\mu_0|}{v'} + 4\pi R^2 \beta\sigma_0 + \frac{1}{2}G(\tau\dot{\gamma})^2 \frac{4}{3}\pi R^3, \quad (1)$$

where $F(R)$ is the free energy of formation of a cluster of radius R, $|\Delta\mu_0|$ is the chemical potential difference between the thermodynamically stable crystal phase and the metastable liquid phase when no shear is applied, (σ_0) is the surface tension or the interfacial free energy of the nucleus at zero shear, (v') is the volume of one molecule in the crystal phase, G is the shear modulus of the nucleus, β is a "shape factor" indicating the shear-induced deformation of the nucleus, and τ is a characteristic time defined as $\tau = (\eta/G)$, where η is the fluid viscosity.

Here, the dimensionless shape factor $\beta = 1 + \frac{7}{24}(\tau\dot{\gamma})^2$ is a correction term to the nucleus surface, which accounts for the volume-preserving change in geometry of the nucleus into an ellipsoid. For perfectly spherical nuclei, β is unity.

Homogeneous nucleation is an activated process, exhibiting a maximum in the free energy at a critical nucleus size N^*. The height of the free energy barrier for nucleation, corresponding to this critical nucleus size N^*, is obtained from

$$F(N^*) = \frac{N_0^*|\Delta\mu_0|}{2} \frac{\beta^3}{[1 - \frac{v'G}{2|\Delta\mu_0|}(\tau\dot{\gamma})^2]^2}, \quad (2)$$

where $N_0^* = [(32\pi\sigma_0^3 v'^2)/(3|\Delta\mu_0|^3)]$ is the critical nucleus size at zero shear.

The steady-state nucleation rate, J, can be estimated using the following familiar CNT-based expression [23]:

$$J = \rho_l Z f^+ e^{-[F(N^*)/k_B T]}, \quad (3)$$

where the nucleation rate J is the current or flux across the free energy barrier, in the cluster-size space and is in units of the number of nucleation events per unit volume per unit time, f^+ is the rate of attachment of particles to the critical cluster, ρ_l is the number density of the supercooled liquid, and Z is the Zeldovich factor. Z captures the probability of multiple recrossings of the energy barrier [29].

The expression for the shear rate-dependent attachment rate f^+ is given by [23]

$$f^+ = \frac{24 D_l}{\lambda^2} \beta (N^*)^{\frac{2}{3}}, \tag{4}$$

where D_l is the two-dimensional diffusion coefficient of the supercooled liquid phase for a particular shear rate and temperature T, and λ is the atomic "jump length," estimated to be about one molecule diameter.

It has been shown earlier that the diffusion coefficient varies linearly with shear rates, at a constant temperature, for the mW model [23]:

$$D_l = D_0 + c\dot{\gamma}, \tag{5}$$

where D_0 is the diffusion coefficient when the shear rate is zero, and c is a fitting parameter with units of squared length. We observe that Eq. (5) holds true for TIP4P/2005, TIP4P/Ice, mW, and LJ. We have estimated c for these systems by fitting D_l, from our nonequilibrium molecular dynamics (NEMD) simulations, to Eq. (5). Such linear behavior is predicted for a suspension of particles, which also provides the following estimate for c [30,31]:

$$c = K_c a^2 \phi, \tag{6}$$

where a is the particle diameter, ϕ is the volume fraction, and K_c is a constant. We have used a value of $K_c = 0.4$, which has been successfully used for suspensions [30] and blood [31]. In this Letter, for hard-sphere colloids, we use Eq (6) to estimate the value of c. D_0 is calculated using the Stokes-Einstein relation, given by $D_0 = (\rho_l)^{\frac{1}{3}}(k_B T/6\eta)$, modified for hard spheres [32].

We note that the shear rates considered in this study are low enough to safely assume that the fluids exhibit Newtonian behavior. Therefore, η has constant values at every temperature, estimated by pinpointing the plateau region independent of applied periodic shear flows, preceding the advent of shear thinning [33]. Further, we assume that the shear modulus G of the nuclei is isotropic, which may not be strictly true for ice. However, the variations in G for both hexagonal ice and amorphous ice are within the range of 3–4.5 GPa [34–36], which do not significantly impact the calculated nucleation rates [23].

The calculation of J in the presence of an applied shear rate $\dot{\gamma}$, at a chosen condition of metastability additionally requires system-specific input quantities, identical to the quintessential seeding method: σ_0, $\Delta\mu_0$, v', ρ_l, and λ. The values of these shear insensitive terms are listed in Tables S1–S3 of the Supplemental Material [37] for water, LJ, and HS, respectively.

The shear-CNT formulation predicts that the nucleation rate J is nonmonotonic in nature with respect to the shear rate, owing to competing energetic and kinetic effects. Equation (2) shows that the free energy barrier will rise with increasing shear rates. Equation (4) indicates that f^+ will increase, due to the increase in both D_l and N^*. The net effect is that of a maximum in J [Eq. (3)] at some particular shear rate.

To analyze the nonmonotonicity, we introduce a min-max normalized [89] nucleation rate, $[(J - J_0)/J_{\max} - J_0]$, defined with respect to J_0, the nucleation rate at zero shear, and $J_{\max}$, the highest nucleation rate observed at a particular temperature [23]. The optimal shear rate, $\dot{\gamma}_{\text{opt}}$, is defined as the shear rate for which $[(J - J_0)/J_{\max} - J_0]$ is maximized.

However, the transcendental nature of the nucleation rate expression prevents us from directly solving an analytical expression for $[(J - J_0)/J_{\max} - J_0]$. In order to further simplify the governing equations of the shear-CNT formalism, we examine the order of magnitudes for the various parameters in the equations involved. For water, LJ, and HS, the shape factor is $\beta \approx 1$ for the highest $\tau\dot{\gamma}$ values considered. For $\dot{\gamma} < (1/\eta)[(2G|\Delta\mu_0|)/v']^{\frac{1}{2}}$, we can use a binomial expansion for the denominator in Eq. (2). Subsequently expanding the exponential in Eq. (3) yields a simplified expression for J:

$$J = J_0 \left(1 + \frac{c}{D_0}\dot{\gamma}\right)\left[1 - \frac{N_0^* v' G}{2 k_B T}(\tau\dot{\gamma})^2\right], \tag{7}$$

where J_0 is the nucleation rate when the shear rate is zero. We note that, although Eq. (7) is cubic in $\dot{\gamma}$, there exists only one positive root and only one positive critical point, $\dot{\gamma}_{\text{opt}}$. This is indicative of a single maximum in J for positive $\dot{\gamma}$.

As the magnitude of the dimensionless term $[(6c^2 G k_B T)/N_0^* v'(D_0\eta)^2]$ is 1 and 2 orders of magnitude lower than unity for the water models and LJ, respectively, we obtain a simplified relation for $\dot{\gamma}_{\text{opt}}$ from Eq. (7) given by

$$\dot{\gamma}_{\text{opt}} = \frac{k_B T G c}{N_0^* D_0 \eta^2 v'}. \tag{8}$$

The following analytical expression for $[(J - J_0)/J_{\max} - J_0]$ can be derived using Eq. (7) and Eq. (8):

$$\frac{J - J_0}{J_{\max} - J_0} = \left(\frac{1}{1 - \frac{c}{D_0}\dot{\gamma}_{\text{opt}}}\right) \times \left(\frac{\dot{\gamma}}{\dot{\gamma}_{\text{opt}}}\right) \times \left[2 - \left(\frac{\dot{\gamma}}{\dot{\gamma}_{\text{opt}}}\right) - \frac{c}{D_0}\dot{\gamma}_{\text{opt}}\left(\frac{\dot{\gamma}}{\dot{\gamma}_{\text{opt}}}\right)^2\right]. \tag{9}$$

This is a cubic polynomial in $\dot{\gamma}/\dot{\gamma}_{\text{opt}}$ of the form $f(x) = ax(2 - x - bx^2)$, where a and b contain the term $(c/D_0)\dot{\gamma}_{\text{opt}}$, and are thus system-dependent constants at a particular condition of metastability. Since the values of b

are in the range of 10^{-4}–10^{-3} for the water models and LJ fluid at various supercoolings, the value of $a = 1/(1-b)$ can be assumed to be unity (Table S9 [37]). For values of $x \leq 2$, corresponding to $\dot{\gamma} \leq 2\dot{\gamma}_{\mathrm{opt}}$, $f(x) = ax(2 - x - bx^2)$ can be approximated by a parabola of the form $x(2-x)$. Hence we observe that, for all the systems studied in this work, parabolic fits approximate the nucleation rate behavior with excellent agreement. A parabolic law, with respect to the dimensionless shear $\dot{\gamma}/\dot{\gamma}_{\mathrm{opt}}$, of the following form can describe the nucleation behavior at a particular temperature (T) and supercooling ΔT:

$$\frac{J - J_0}{J_{\mathrm{max}} - J_0} = 1 - \left(\frac{\dot{\gamma}}{\dot{\gamma}_{\mathrm{opt}}} - 1\right)^2. \tag{10}$$

The vertex of this parabola is at unity. We recover a family of parabolas with vertices at $\dot{\gamma}_{\mathrm{opt}}$, at every temperature, if $[(J - J_0)/J_{\mathrm{max}} - J_0]$ is plotted against $\dot{\gamma}$.

Figure 1 depicts the universal nature of the nonmonotonicity of the normalized nucleation rate, generated by the superposition of available data for the water models, LJ fluid, and hard spheres. These include our results (see Secs. 3 and 4 of the Supplemental Material [37] for details of input parameters), as well as those of earlier studies by other groups [13,22]. We infer the existence of a single maximum nucleation rate, at any given metastability, for every system. For shear rates higher than $\dot{\gamma}_{\mathrm{opt}}$), the

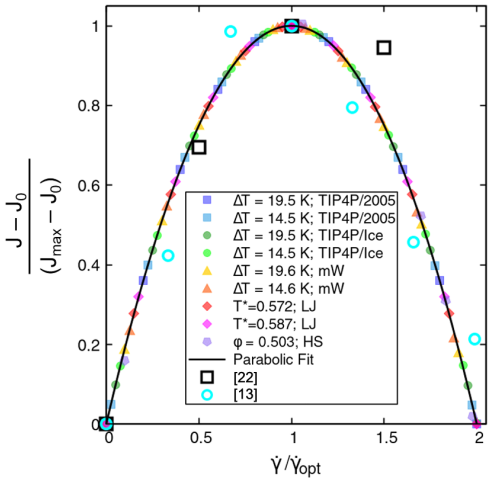

FIG. 1. Variation of the normalized nucleation rate with the normalized shear rate, $\dot{\gamma}/\dot{\gamma}_{\mathrm{opt}}$ at selected metastabilities, plotted alongside the corresponding parabolic fit. Equation (10) has been denoted by a solid black line, and filled markers symbolize the nucleation rates calculated using shear-CNT for various systems and metastabilities. Black open squares show the data for the mW model estimated by Luo *et al.* [22], for a supercooling of 67.6 K, using brute-force approaches to calculate and fit to the induction times [90]. Errors associated with J were within 10% [22]. Open turquoise circles depict the data for a sheared two-dimensional Ising model, obtained using forward-flux sampling [91], by Allen *et al.* [13]. Error bars for J were of the range of 7%–10% [13].

nucleation rate decreases. Despite the complex interactions of shear-dependent terms in Eq. (3), the simple functional form of Eq. (10) works well for the systems considered. These results indicate that this behavior is fundamental to Newtonian fluids obeying CNT.

A previous study on the mW model suggests that the shear-dependent nucleation rates have a nonlinear dependence on the temperature [23]. This could arise from the inclusion of several temperature-dependent parameters in the expression for the nucleation rate [Eq. (3)]. Scrutiny of Eq. (1), Eq. (2), and Eq. (4) reveals the recurring dimensionless group $\tau\dot{\gamma}$. The temperature dependence of the nucleation behavior under shear is embodied by the dimensionless product, $\tau\dot{\gamma}_{\mathrm{opt}}$, where $\dot{\gamma}_{\mathrm{opt}}$ [Eq. (8)] depends on the temperature as well as the nature of the system.

Rearranging the terms in the simplified relation for $\dot{\gamma}$ in Eq. (8), we obtain the following expression for the dimensionless $\tau\dot{\gamma}$:

$$\tau\dot{\gamma}_{\mathrm{opt}} = \left(\frac{k_B T}{D_0 \eta}\frac{c}{v'}\right) \times \frac{1}{N_0^*}, \tag{11}$$

where we define $B = (k_B T/D_0\eta)(c/v')$, which is a dimensionless group related to the transport properties. N_0^* is dependent on the thermodynamic properties.

To compare the behavior of the water models and LJ fluid, we define the percent supercooling with respect to the melting point, T_m, for each model. The percent supercooling can be considered to be a driving force for nucleation [92]. Temperature relations are obtained for η and D_0 using power law fits. Second-order polynomials suffice to approximate the densities [93]. Linear fits to σ_0 [93], $|\Delta\mu_0|$, c, are used to obtain the predicted values of each variable as a function of temperature.

Figure 2(a) shows the variation in $\tau\dot{\gamma}_{\mathrm{opt}}$ with percent supercooling for the water models and LJ. The simplified Eq. (11) performs well for the models considered [denoted by solid lines in Fig. 2(a)]. $\tau\dot{\gamma}_{\mathrm{opt}}$ exhibits a single maximum for every water model. In particular, the rigid water models show nearly identical behavior. We also note that every system shows monotonic increase in the limit of 10% supercooling. However, the $\tau\dot{\gamma}_{\mathrm{opt}}$ curve for LJ shows a qualitatively different trend compared to the water models at higher supercoolings.

Figure 2(b) depicts the dependence of the dimensionless group B on the percent supercooling. The nonmonotonic behavior of B for the water models closely mirrors that of $\tau\dot{\gamma}_{\mathrm{opt}}$ in Fig. 2(a). Concomitantly, we attribute the trend in $\tau\dot{\gamma}_{\mathrm{opt}}$ for LJ to the monotonic behavior of B. The inset of Fig 2(b) shows a nearly universal trend of N_0^* with percent supercooling.

Furthermore, our analysis shows that the origin of the divergent trends in B [Fig. 2(b)] lies in the Stokes-Einstein (SE) relation. Anomalous transport properties of supercooled liquids are often characterized by SE violation

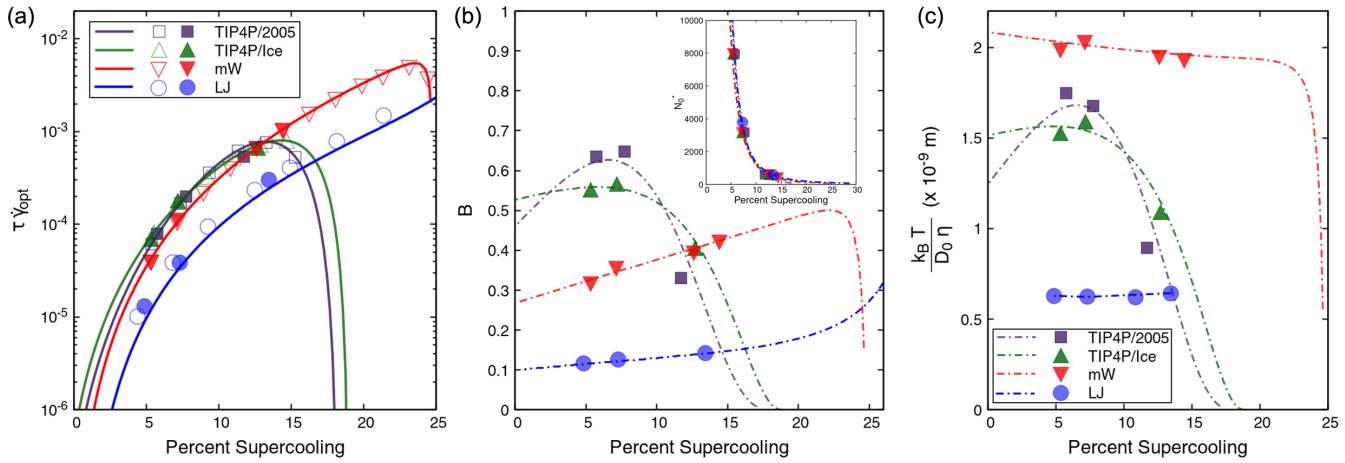

FIG. 2. (a) Dependence of $\tau\dot{\gamma}_{\mathrm{opt}}$ on the percent supercooling, $[(T_m - T)/T_m)] \times 100\%$, for TIP4P/2005, TIP4P/Ice, mW, and LJ. Filled and open markers represent values calculated using shear-CNT, with input data calculated from simulations and with approximated inputs, respectively. The solid lines denote $\tau\dot{\gamma}_{\mathrm{opt}}$ estimated using the simplified theory, Eq. (11). (b) Variation of $B = [(k_BT/D_0\eta)(c/v')]$ with the percent supercooling. The inset shows N_0^* plotted against the percent supercooling. (c) Test of the Stokes-Einstein (SE) relation, according to which $(k_BT/D_0\eta)$ should be constant. SE relation is clearly violated for the water models for the supercoolings considered. Data for which the values of η, D_0, c and v' were calculated using simulation data are denoted by filled markers, and dashed lines show values calculated using approximations.

[94–102]. According to the SE relation, the following expression holds true at all temperatures [103,104]:

$$D_0 \propto \frac{k_BT}{\eta}, \tag{12}$$

which implies that, if the SE relation is valid, the term $(k_BT/D_0\eta)$ is constant.

Figure 2(c) depicts the variation of $(k_BT/D_0\eta)$ with percent supercooling. The SE relation breaks down spectacularly for supercooled water [102,105–107], as shown by maxima in the $(k_BT/D_0\eta)$ curves for TIP4P/2005, TIP4P/Ice and mW. These are directly reflected by the maxima of B and $\tau\dot{\gamma}_{\mathrm{opt}}$ for the water models. In contrast, $(k_BT/D_0\eta)$ is relatively constant for LJ [Fig. 2(c)], which suggests that the SE relation is preserved, in the case of the LJ fluid, for the supercoolings considered in this work. We surmise that the temperature dependence of the nucleation behavior is strongly linked to the violation or preservation of the SE relation, and thus depends significantly on the behavior of flow properties. The decoupling of D_0 and η, typified by the SE violation, is thought to originate from spatial heterogeneities in the dynamics of strongly supercooled glass-forming liquids [94,98,100,102,107–109].

In conclusion, we have reported the effects of shear on the nucleation rates at different temperatures, for the TIP4P/2005, TIP4P/Ice, mW water models, LJ fluid, and HS colloids. Nucleation events at low and moderate supercoolings are notoriously difficult to simulate, and such extensive calculations are virtually intractable using brute-force molecular dynamics. By employing the shear-CNT formalism, based on modified CNT equations, we were able to obtain nucleation rate curves for several metastable conditions.

In accordance with previous simulation results for colloids, glassy systems, the Ising model, and mW water [13,16,17,22,23], we confirmed that the nucleation rate curves exhibit nonmonotonic behavior with shear, at a particular supercooling. To rationalize this nonmonotonicity with shear, we derived a simplified theory describing the governing equations of shear CNT. We generated a "universal" curve for the normalized nucleation rate $[(J - J_0)/J_{\max} - J_0]$ with $\dot{\gamma}/\dot{\gamma}_{\mathrm{opt}}$. We infer that the existence of a maximum in the nucleation rate with shear is a universal property of systems that follow CNT.

We systematically investigated the temperature dependence of the nucleation rate curves for TIP4P/2005, TIP4P/Ice, mW, and LJ by examining the behavior of the dimensionless group $\tau\dot{\gamma}_{\mathrm{opt}}$. An approximate relation for $\tau\dot{\gamma}_{\mathrm{opt}}$ was obtained, expressed as a product of two dimensionless groups: B, which is related to transport properties, and the thermodynamic quantity $1/N_0^*$. The analysis reveals that the behavior of $\tau\dot{\gamma}_{\mathrm{opt}}$ is solely determined by the nature of B. The anomalous temperature dependence of the nucleation behavior of water originates from the SE violation. We discovered that universal behavior is recovered for N_0^*, for every system.

Thus, we have uncovered underlying commonalities and determined the origin of anomalies in the nucleation behavior for several supercooled molecular systems under shear. Our results provide insight into the previously unexplored, intriguingly complex interplay of temperature and shear, affecting the nucleation rate.

This work was supported by the Science and Engineering Research Board (sanction number STR/2019/000090 and

CRG/2019/001325). Computational resources were provided by the HPC cluster of the Computer Center (CC), Indian Institute of Technology Kanpur.

*indrasd@iitk.ac.in
†jayantks@iitk.ac.in

[1] G. C. Sosso, J. Chen, S. J. Cox, M. Fitzner, P. Pedevilla, A. Zen, and A. Michaelides, Crystal nucleation in liquids: Open questions and future challenges in molecular dynamics simulations, Chem. Rev. **116**, 7078 (2016).
[2] R. Blaak, S. Auer, D. Frenkel, and H. Löwen, Crystal Nucleation of Colloidal Suspensions under sshear, Phys. Rev. Lett. **93**, 068303 (2004).
[3] R. Blaak, S. Auer, D. Frenkel, and H. Löwen, Homogeneous nucleation of colloidal melts under the influence of shearing fields, J. Phys. Condens. Matter **16**, S3873 (2004).
[4] A. V. Mokshin and J.-L. Barrat, Shear induced structural ordering of a model metallic glass, J. Chem. Phys. **130**, 034502 (2009).
[5] R. S. Graham and P. D. Olmsted, Coarse-Grained Simulations of Flow-Induced Nucleation in Semicrystalline Polymers, Phys. Rev. Lett. **103**, 115702 (2009).
[6] M. Radu and T. Schilling, Solvent hydrodynamics speed up crystal nucleation in suspensions of hard spheres, Europhys. Lett. **105**, 26001 (2014).
[7] C. Forsyth, P. A. Mulheran, C. Forsyth, M. D. Haw, I. S. Burns, and J. Sefcik, Influence of controlled fluid shear on nucleation rates in glycine aqueous solutions, Cryst. Growth Des. **15**, 94 (2015).
[8] Z. Shao, J. P. Singer, Y. Liu, Z. Liu, H. Li, M. Gopinadhan, and C. S. O'Hern, J. Schroers, and C. O. Osuji, Shear-accelerated crystallization in a supercooled atomic liquid, Phys. Rev. E **91**, 020301 (2015).
[9] J. Ruiz-Franco, J. Marakis, N. Gnan, J. Kohlbrecher, M. Gauthier, M. Lettinga, D. Vlassopoulos, and E. Zaccarelli, Crystal-to-Crystal Transition of Ultrasoft Colloids under Shear, Phys. Rev. Lett. **120**, 078003 (2018).
[10] S. Stroobants, M. Callewaert, M. Krzek, S. Chinnu, P. Gelin, I. Ziemecka, J. F. Lutsko, W. D. Malsche, and D. Maes, Influence of shear on protein crystallization under constant shear conditions, Cryst. Growth Des. **20**, 1876 (2020).
[11] P. Holmqvist, M. P. Lettinga, J. Buitenhuis, and J. K. G. Dhont, Crystallization kinetics of colloidal spheres under stationary shear flow, Langmuir **21**, 10976 (2005).
[12] J. Liu and Å. C. Rasmuson, Influence of agitation and fluid shear on primary nucleation in solution, Cryst. Growth Des. **13**, 4385 (2013).
[13] R. J. Allen, C. Valeriani, S. Tănase-Nicola, P. R. ten Wolde, and D. Frenkel, Homogeneous nucleation under shear in a two-dimensional ising model: Cluster growth, coalescence, and breakup, J. Chem. Phys. **129**, 134704 (2008).
[14] J. J. Cerdà, T. Sintes, C. Holm, C. M. Sorensen, and A. Chakrabarti, Shear effects on crystal nucleation in colloidal suspensions, Phys. Rev. E **78**, 031403 (2008).
[15] B. Lander, U. Seifert, and T. Speck, Crystallization in a sheared colloidal suspension, J. Chem. Phys. **138**, 224907 (2013).
[16] D. Richard and T. Speck, The role of shear in crystallization kinetics: From suppression to enhancement, Sci. Rep. **5**, 14610 (2015).
[17] F. Mura and A. Zaccone, Effects of shear flow on phase nucleation and crystallization, Phys. Rev. E **93**, 042803 (2016).
[18] D. Richard and T. Speck, Classical nucleation theory for the crystallization kinetics in sheared liquids, Phys. Rev. E **99**, 062801 (2019).
[19] A. V. Mokshin and J.-L. Barrat, Crystal nucleation and cluster-growth kinetics in a model glass under shear, Phys. Rev. E **82**, 021505 (2010).
[20] A. V. Mokshin, B. N. Galimzyanov, and J.-L. Barrat, Extension of classical nucleation theory for uniformly sheared systems, Phys. Rev. E **87**, 062307 (2013).
[21] H. L. Peng, D. M. Herlach, and T. Voigtmann, Crystal growth in fluid flow: Nonlinear response effects, Phys. Rev. Mater. **1**, 030401 (2017).
[22] S. Luo, J. Wang, and Z. Li, Homogeneous ice nucleation under shear, J. Phys. Chem. B **124**, 3701 (2020).
[23] A. Goswami, I. S. Dalal, and J. K. Singh, Seeding method for ice nucleation under shear, J. Chem. Phys. **153**, 094502 (2020).
[24] L. G. M. Pettersson, R. H. Henchman, and A. Nilsson, Water—the most anomalous liquid, Chem. Rev. **116**, 7459 (2016).
[25] J. L. F. Abascal and C. Vega, A general purpose model for the condensed phases of water: TIP4p/2005, J. Chem. Phys. **123**, 234505 (2005).
[26] J. L. F. Abascal, E. Sanz, R. G. Fernández, and C. Vega, A potential model for the study of ices and amorphous water: TIP4p/ice, J. Chem. Phys. **122**, 234511 (2005).
[27] V. Molinero and E. B. Moore, Water modeled as an intermediate element between carbon and silicon, J. Phys. Chem. B **113**, 4008 (2009).
[28] J. Broughton and G. Gilmer, Surface free energy and stress of a Lennard-Jones crystal, Acta Metall. **31**, 845 (1983).
[29] A. C. Pan and D. Chandler, Dynamics of nucleation in the Ising model†, J. Phys. Chem. B **108**, 19681 (2004).
[30] I. Siqueira, R. Rebouças, and M. Carvalho, Migration and alignment in the flow of elongated particle suspensions through a converging-diverging channel, J. Non-Newtonian Fluid Mech. **243**, 56 (2017).
[31] K. Chandran, I. S. Dalal, K. Tatsumi, and K. Muralidhar, Numerical simulation of blood flow modeled as a fluid-particulate mixture, J. Non-Newtonian Fluid Mech. **285**, 104383 (2020).
[32] N. Ohtori, H. Uchiyama, and Y. Ishii, The Stokes-Einstein relation for simple fluids: From hard-sphere to Lennard-Jones via WCA potentials, J. Chem. Phys. **149**, 214501 (2018).
[33] B. Hess, Determining the shear viscosity of model liquids from molecular dynamics simulations, J. Chem. Phys. **116**, 209 (2002).
[34] T. Loerting and N. Giovambattista, Amorphous ices: Experiments and numerical simulations, J. Phys. Condens. Matter **18**, R919 (2006).
[35] P. Cao, J. Wu, Z. Zhang, B. Fang, L. Peng, T. Li, T. J. H. Vlugt, and F. Ning, Mechanical properties of bi- and polycrystalline ice, AIP Adv. **8**, 125108 (2018).

[36] P. A. F. P. Moreira, R. G. de Aguiar Veiga, and M. de Koning, Elastic constants of ice ih as described by semi-empirical water models, J. Chem. Phys. **150**, 044503 (2019).
[37] See Supplemental Material http://link.aps.org/supplemental/10.1103/PhysRevLett.126.195702for further details of supporting calculations, simulations, and fits reported, which includes Refs. [38–88].
[38] S. Plimpton, Fast parallel algorithms for short-range molecular dynamics, J. Comput. Phys. **117**, 1 (1995).
[39] D. J. Evans and G. P. Morriss, Nonlinear-response theory for steady planar couette flow, Phys. Rev. A **30**, 1528 (1984).
[40] A. W. Lees and S. F. Edwards, The computer study of transport processes under extreme conditions, J. Phys. C **5**, 1921 (1972).
[41] P. J. Daivis and B. D. Todd, A simple, direct derivation and proof of the validity of the SLLOD equations of motion for generalized homogeneous flows, J. Chem. Phys. **124**, 194103 (2006).
[42] W. Shinoda, M. Shiga, and M. Mikami, Rapid estimation of elastic constants by molecular dynamics simulation under constant stress, Phys. Rev. B **69**, 134103 (2004).
[43] J. W. E. R. W Hockney, *Computer Simulation Using Particles* (CRC Press, Boca Raton, 1988).
[44] J.-P. Ryckaert, G. Ciccotti, and H. J. Berendsen, Numerical integration of the Cartesian equations of motion of a system with constraints: Molecular dynamics of n-alkanes, J. Comput. Phys. **23**, 327 (1977).
[45] T. Giorgino, Computing diffusion coefficients in macromolecular simulations: The diffusion coefficient tool for VMD, J. Open Source Software **4**, 1698 (2019).
[46] J. R. Espinosa, E. Sanz, C. Valeriani, and C. Vega, Homogeneous ice nucleation evaluated for several water models, J. Chem. Phys. **141**, 18C529 (2014).
[47] D. P. Woodruff, *The Solid–Liquid Interface* (Cambridge University Press, Cambridge, England, 1973).
[48] K. F. Kelton, A. L. Greer, and C. V. Thompson, Transient nucleation in condensed systems, J. Chem. Phys. **79**, 6261 (1983).
[49] K. Kelton, Crystal nucleation in liquids and glasses, in *Solid State Physics* (Elsevier, New York, 1991), pp. 75–177.
[50] M. Volmer and A. Weber, Nucleus formation in supersaturated systems, Z. Phys. Chem. **119**, 277 (1926).
[51] R. Becker and W. Döring, Kinetische behandlung der keimbildung in übersättigten dämpfen, Ann. Phys. (Leipzig) **416**, 719 (1935).
[52] 10. On the theory of new phase formation. cavitation, in *Selected Works of Yakov Borisovich Zeldovich*, edited by R. A. Sunyaev (Princeton University Press, Princeton, 1992), Vol. I, pp. 120–137.
[53] S. Auer and D. Frenkel, Quantitative prediction of crystal-nucleation rates for spherical colloids: A computational approach, Annu. Rev. Phys. Chem. **55**, 333 (2004).
[54] S. Auer and D. Frenkel, Prediction of absolute crystal-nucleation rate in hard-sphere colloids, Nature (London) **409**, 1020 (2001).
[55] S. Auer and D. Frenkel, Numerical prediction of absolute crystallization rates in hard-sphere colloids, J. Chem. Phys. **120**, 3015 (2004).
[56] X.-M. Bai and M. Li, Test of classical nucleation theory via molecular-dynamics simulation, J. Chem. Phys. **122**, 224510 (2005).
[57] B. C. Knott, V. Molinero, M. F. Doherty, and B. Peters, Homogeneous nucleation of methane hydrates: Unrealistic under realistic conditions, J. Am. Chem. Soc. **134**, 19544 (2012).
[58] E. Sanz, C. Vega, J. R. Espinosa, R. Caballero-Bernal, J. L. F. Abascal, and C. Valeriani, Homogeneous ice nucleation at moderate supercooling from molecular simulation, J. Am. Chem. Soc. **135**, 15008 (2013).
[59] R. G. Pereyra, I. Szleifer, and M. A. Carignano, Temperature dependence of ice critical nucleus size, J. Chem. Phys. **135**, 034508 (2011).
[60] J. R. Espinosa, C. Vega, C. Valeriani, and E. Sanz, The crystal-fluid interfacial free energy and nucleation rate of NaCl from different simulation methods, J. Chem. Phys. **142**, 194709 (2015).
[61] N. E. R. Zimmermann, B. Vorselaars, D. Quigley, and B. Peters, Nucleation of NaCl from aqueous solution: Critical sizes, ion-attachment kinetics, and rates, J. Am. Chem. Soc. **137**, 13352 (2015).
[62] X.-M. Bai and M. Li, Calculation of solid-liquid interfacial free energy: A classical nucleation theory based approach, J. Chem. Phys. **124**, 124707 (2006).
[63] D. J. Quesnel, D. S. Rimai, and L. P. DeMejo, Elastic compliances and stiffnesses of the fcc Lennard-Jones solid, Phys. Rev. B **48**, 6795 (1993).
[64] C. Feldman and M. L. Klein, On the elastic constants of polycrystalline argon, Philos. Mag. **17**, 135 (1968).
[65] U. Gasser, Real-space imaging of nucleation and growth in colloidal crystallization, Science **292**, 258 (2001).
[66] W. Sandberg and D. Heyes, Self-diffusion in equilibrium and sheared liquid mixtures by molecular dynamics, Mol. Phys. **85**, 635 (1995).
[67] D. L. Malandro and D. J. Lacks, Molecular-Level Mechanical Instabilities and Enhanced Self-Diffusion in Flowing Liquids, Phys. Rev. Lett. **81**, 5576 (1998).
[68] E. Cussler, *Diffusion: Mass Transfer in Fluid Systems* (Cambridge University Press, Cambridge, England, 2009).
[69] Z. Li, Critical particle size where the Stokes-Einstein relation breaks down, Phys. Rev. E **80**, 061204 (2009).
[70] K. R. Harris and L. A. Woolf, Temperature and volume dependence of the viscosity of water and heavy water at low temperatures, J. Chem. Eng. Data **49**, 1064 (2004).
[71] M. A. González and J. L. F. Abascal, The shear viscosity of rigid water models, J. Chem. Phys. **132**, 096101 (2010).
[72] Y. A. Osipov, B. V. Zheleznyi, and N. F. Bondarenko, The shear viscosity of water supercooled to −35°C, J. Phys. Chem. **51**, 748 (1977).
[73] A. Dehaoui, B. Issenmann, and F. Caupin, Viscosity of deeply supercooled water and its coupling to molecular diffusion, Proc. Natl. Acad. Sci. U.S.A. **112**, 12020 (2015).
[74] J. Qvist, C. Mattea, E. P. Sunde, and B. Halle, Rotational dynamics in supercooled water from nuclear spin relaxation and molecular simulations, J. Chem. Phys. **136**, 204505 (2012).

[75] S. H. Lee and J. Kim, Transport properties of bulk water at 243–550 k: A comparative molecular dynamics simulation study using SPC/e, TIP4p, and TIP4p/2005 water models, Mol. Phys. **117**, 1926 (2019).
[76] R. J. Speedy and C. A. Angell, Isothermal compressibility of supercooled water and evidence for a thermodynamic singularity at −45°C, J. Chem. Phys. **65**, 851 (1976).
[77] E. Leutheusser, Dynamical model of the liquid-glass transition, Phys. Rev. A **29**, 2765 (1984).
[78] W. Gotze and L. Sjogren, Relaxation processes in supercooled liquids, Rep. Prog. Phys. **55**, 241 (1992).
[79] F. Sciortino, Slow dynamics in supercooled water, Chem. Phys. **258**, 307 (2000).
[80] O. Mishima and H. E. Stanley, The relationship between liquid, supercooled and glassy water, Nature (London) **396**, 329 (1998).
[81] P. H. Handle, T. Loerting, and F. Sciortino, Supercooled and glassy water: Metastable liquid(s), amorphous solid(s), and a no-man's land, Proc. Natl. Acad. Sci. U.S.A. **114**, 13336 (2017).
[82] K. H. Kim, A. Späh, H. Pathak, F. Perakis, D. Mariedahl, K. Amann-Winkel, J. A. Sellberg, J. H. Lee, S. Kim, J. Park, K. H. Nam, T. Katayama, and A. Nilsson, Maxima in the thermodynamic response and correlation functions of deeply supercooled water, Science **358**, 1589 (2017).
[83] Y. Ni, N. J. Hestand, and J. L. Skinner, Communication: Diffusion constant in supercooled water as the widom line is crossed in no man's land, J. Chem. Phys. **148**, 191102 (2018).
[84] S. Saito and B. Bagchi, Thermodynamic picture of vitrification of water through complex specific heat and entropy: A journey through "no man's land", J. Chem. Phys. **150**, 054502 (2019).
[85] J. H. ter Horst and D. Kashchiev, Determination of the nucleus size from the growth probability of clusters, J. Chem. Phys. **119**, 2241 (2003).
[86] P. Yi, C. R. Locker, and G. C. Rutledge, Molecular dynamics simulation of homogeneous crystal nucleation in polyethylene, Macromolecules **46**, 4723 (2013).
[87] C. Vega and J. L. F. Abascal, Relation between the melting temperature and the temperature of maximum density for the most common models of water, J. Chem. Phys. **123**, 144504 (2005).
[88] R. L. Davidchack and B. B. Laird, Direct calculation of the crystal–melt interfacial free energies for continuous potentials: Application to the lennard-jones system, J. Chem. Phys. **118**, 7651 (2003).
[89] D. Freedman, R. Pisani, and R. Purves, *Statistics* (Norton & Company, New York, 2018).
[90] M. Fitzner, G. C. Sosso, S. J. Cox, and A. Michaelides, The many faces of heterogeneous ice nucleation: Interplay between surface morphology and hydrophobicity, J. Am. Chem. Soc. **137**, 13658 (2015).
[91] R. J. Allen, P. B. Warren, and P. R. ten Wolde, Sampling Rare Switching Events in Biochemical Networks, Phys. Rev. Lett. **94**, 018104 (2005).
[92] X. Liu, K. Zhuang, S. Lin, Z. Zhang, and X. Li, Determination of supercooling degree, nucleation and growth rates, and particle size for ice slurry crystallization in vacuum, Crystals **7**, 128 (2017).
[93] J. R. Espinosa, C. Vega, C. Valeriani, and E. Sanz, Seeding approach to crystal nucleation, J. Chem. Phys. **144**, 034501 (2016).
[94] J. A. Hodgdon and F. H. Stillinger, Stokes-Einstein violation in glass-forming liquids, Phys. Rev. E **48**, 207 (1993).
[95] F. H. Stillinger, A topographic view of supercooled liquids and glass formation, Science **267**, 1935 (1995).
[96] G. Tarjus and D. Kivelson, Breakdown of the Stokes–Einstein relation in supercooled liquids, J. Chem. Phys. **103**, 3071 (1995).
[97] M. T. Cicerone and M. D. Ediger, Relaxation of spatially heterogeneous dynamic domains in supercooled ortho-terphenyl, J. Chem. Phys. **103**, 5684 (1995).
[98] M. D. Ediger, Spatially heterogeneous dynamics in supercooled liquids, Annu. Rev. Phys. Chem. **51**, 99 (2000).
[99] Z. Shi, P. G. Debenedetti, and F. H. Stillinger, Relaxation processes in liquids: Variations on a theme by Stokes and Einstein, J. Chem. Phys. **138**, 12A526 (2013).
[100] S. Sengupta, S. Karmakar, C. Dasgupta, and S. Sastry, Breakdown of the Stokes-Einstein relation in two, three, and four dimensions, J. Chem. Phys. **138**, 12A548 (2013).
[101] P. Henritzi, A. Bormuth, F. Klameth, and M. Vogel, A molecular dynamics simulations study on the relations between dynamical heterogeneity, structural relaxation, and self-diffusion in viscous liquids, J. Chem. Phys. **143**, 164502 (2015).
[102] T. Kawasaki and K. Kim, Identifying time scales for violation/preservation of Stokes-Einstein relation in supercooled water, Sci. Adv. **3**, e1700399 (2017).
[103] W. Sutherland, LXXV. A dynamical theory of diffusion for non-electrolytes and the molecular mass of albumin, London, Edinburgh, Dublin Philos. Mag. J. Sci. **9**, 781 (1905).
[104] J. T. Hynes, Statistical mechanics of molecular motion in dense fluids, Annu. Rev. Phys. Chem. **28**, 301 (1977).
[105] S.-H. Chen, F. Mallamace, C.-Y. Mou, M. Broccio, C. Corsaro, A. Faraone, and L. Liu, The violation of the Stokes-Einstein relation in supercooled water, Proc. Natl. Acad. Sci. U.S.A. **103**, 12974 (2006).
[106] L. Xu, F. Mallamace, Z. Yan, F. W. Starr, S. V. Buldyrev, and H. E. Stanley, Appearance of a fractional Stokes–Einstein relation in water and a structural interpretation of its onset, Nat. Phys. **5**, 565 (2009).
[107] T. Kawasaki and K. Kim, Spurious violation of the Stokes–Einstein–Debye relation in supercooled water, Sci. Rep. **9**, 8118 (2019).
[108] F. H. Stillinger and J. A. Hodgdon, Translation-rotation paradox for diffusion in fragile glass-forming liquids, Phys. Rev. E **50**, 2064 (1994).
[109] T. G. Lombardo, P. G. Debenedetti, and F. H. Stillinger, Computational probes of molecular motion in the Lewis-Wahnström model for ortho-terphenyl, J. Chem. Phys. **125**, 174507 (2006).